The Journal of Neuroscience, April 1995, 15(4): 2638–2655

# Physiological Subgroups of Nonpyramidal Cells with Specific Morphological Characteristics in Layer II/III of Rat Frontal Cortex

**Yasuo Kawaguchi**

Laboratory for Neural Circuits, Bio-Mimetic Control Research Center, The Institute of Physical and Chemical Research (RIKEN), Atsuta, Nagoya 456 Japan

**Physiological and morphological properties of nonpyramidal cells in layer II/III of frontal cortex of young rats were studied *in vitro* by whole-cell recording and intracellular staining with biocytin. Layer II/III nonpyramidal cells could be divided into four subgroups by their firing patterns in response to depolarizing current pulses and their patterns of dendritic and axonal arborizations. (1) Fast-spiking (FS) cells (35% of the total sample) showed an abrupt episode of nonadapting repetitive discharges of shorter-duration action potentials. FS cells had local and horizontal axonal arbors which did not enter layer I. This type of FS cell was immunoreactive for parvalbumin and included some basket cells. Three chandelier cells were identified as FS cells, although one chandelier cell was not identified as an FS cell. (2) Late-spiking (LS) cells (11%) exhibited slowly developing ramp depolarizations near threshold. LS cells were neurogliaform cells. (3) Low-threshold spike (LTS) cells (5%) had prominent low-threshold spikes when stimulated from hyperpolarizations. The main axons of LTS cells ascended, and the collaterals entered into layer I. (4) The remaining cells [regular-spiking nonpyramidal (RSNP) cells] (49%) could not be categorized into the above three subgroups. In some RSNP cells depolarizing pulses from hyperpolarizations induced fast depolarizing notches with small amplitude. RSNP cells had vertically elongated axonal fields, extending from layer I to V, sometimes to layer VI. This subgroup included double bouquet cells and bipolar cells. Each subgroup with a different firing mode may differentially contribute to neocortical laminar and columnar circuitry.**

***[Key words: nonpyramidal cell, basket cell, chandelier cell, neurogliaform cell, double bouquet cell, bipolar cell, fast-spiking cell, low-threshold spike, parvalbumin, neocortex, frontal cortex]***

Mammalian neocortical neurons are broadly divided into two major groups: pyramidal cells with spiny dendrites and nonpyramidal cells with sparsely spiny dendrites (Peters and Jones, 1984). While pyramidal cells are excitatory projection cells in neocortex, most nonpyramidal cells are considered to be GABAergic inhibitory interneurons (Houser et al., 1983). Previous *in vitro* studies have shown heterogeneity of firing properties in pyramidal cells, but only one type of firing pattern in nonpyramidal cells (McCormick et al., 1985; Connors and Gutnick, 1990). This was surprising since nonpyramidal cells are morphologically much more diverse than pyramidal cells (Peters and Jones, 1984).

Recently it was recognized that the morphological heterogeneity of nonpyramidal cells has at least some electrophysiological counterpart in layer V of rat frontal cortex. Fast-spiking cells (FS cells) have exceptionally brief action potentials and fast, nonadapting patterns of firing. Low-threshold spike cells (LTS cells) generate low-threshold spikes from hyperpolarized potentials in response to depolarization (Foehring et al., 1991; Kawaguchi, 1993). FS and LTS nonpyramidal cells in layer V also have distinct morphologies and immunohistochemical characteristics: (1) FS cells have axonal arborizations that are more dense near their somata and are oriented horizontally, and they express the calcium-binding protein parvalbumin; and (2) LTS cells have more vertical axonal arborizations, extending up to layer I, and exhibit calbindin $D_{28k}$ immunoreactivity (Kawaguchi, 1993; Kawaguchi and Kubota, 1993, 1995). Both types of nonpyramidal cells are considered to be GABAergic (Celio, 1986; Hendry et al., 1989; Kawaguchi and Kubota, 1993; Kubota et al.,1994). These observations suggest that GABAergic nonpyramidal cells in neocortex can be divided into several functional groups on the basis of firing modes, axonal distributions, and chemical properties.

The present study attempts to extend those previous results to the upper layers, where nonpyramidal cells and GABA-immunoreactive cells are in greater concentration and more numerous than in lower layers (Peters et al., 1985; Hendry et al., 1987; Kubota et al., 1994) and where there is also an even larger morphological diversity among nonpyramidal cells (Fairén et al., 1984). It is shown that nonpyramidal cells in layer II/III are physiologically more diverse than previously described in layer V (Kawaguchi, 1993), but physiological properties generally correlate with specific morphological characteristics, implying specific contributions of different subgroups to the laminar and columnar circuitry of the cortex.

## Materials and Methods

The physiological, histological, and immunohistochemical procedures used have been previously described in detail (Kawaguchi, 1992, 1993; Kawaguchi and Kubota, 1993).

In vitro *slice preparation and solutions used.* The experiments were performed on young Wistar rats (18–22 d postnatal). Animals were deeply anesthetized with ether and decapitated, and the brains quickly removed, submerged in ice-cold physiological Ringer's solution, and

Received Mar. 14, 1994; revised Oct. 6, 1994; accepted Oct. 13, 1994.

This work was supported by the Frontier Research Program. I thank Ariel Agmon, Tsutomu Hashikawa, and Yoshiyuki Kubota for discussion and comments on the manuscript.

Correspondence should be addressed to Yasuo Kawaguchi, Laboratory for Neural Circuits, Bio-Mimetic Control Research Center (RIKEN), 3-8-31 Rokuban, Atsuta, Nagoya 456 Japan.

hemisected. One hundred eighty to two hundred micrometer thick sections including the medial agranular cortex (Fr2) (Donoghue and Wise, 1982; Zilles and Wree, 1985) were cut on a Microslicer (Dosaka EM) in a plane oblique to the horizontal. Slices were then incubated in oxygenated Ringer's solution at a temperature of 29–30°C for 1–2 hr. The standard Ringer's solution had the following composition (in mM): NaCl, 124.0; KCl, 3.0; $CaCl_2$, 2.4; $MgCl_2$, 1.3; $NaHCO_3$, 26.0; $NaH_2PO_4$, 1.0; and glucose, 10.0, and was continuously bubbled with a mixture of 95% $O_2$ and 5% $CO_2$. After incubation, a single slice was transferred to a recording chamber placed on the stage of an upright microscope, and was totally submerged in the superfusing medium at 29–30°C. The remaining slices were kept in a holding chamber containing oxygenated Ringer's solution at 26–27°C.

*Whole-cell recording and stimulation.* The somata of individual neocortical cells were visualized using a 40× water-immersion objective (Zeiss). Pyramidal-like cells were identified by their somatic shape and visualization of the bases of apical dendrites arising from the pial side of the soma, and were preferentially excluded. Layer II/III cells without apparent apical dendrites were preferentially targeted in order to obtain a larger sample of nonpyramidal cells. Recorded cells were identified as pyramidal or nonpyramidal cells by subsequent intracellular staining. Whole-cell recordings with a high seal resistance (more than 2 GΩ before break-in) were obtained from cells close to the surface of the slices without prior cleaning.

Electrodes were fabricated from borosilicate glass pipettes (o.d. 1.5 mm) and filled with a solution consisting of potassium-methylsulfate 120 mM, EGTA 0.6 mM, $MgCl_2$ 2.0 mM, ATP 4.0 mM, GTP 0.3 mM, HEPES 10 mM, and biocytin (Sigma, 0.5%). Pipette resistances were 4–5 MΩ. Recordings were made by conventional bridge-balance and capacitance neutralization techniques using intracellular amplifier (IR-283, Neuro Data Instruments). Neural signals were viewed on an oscilloscope and stored on computer (Macintosh Quadra 700) using interface (ITC-16, Instrutech Corporation) and software (AXODATA, Axon Instruments). Data were analyzed by computer software (AXOGRAPH, Axon Instruments). Several apparent parameters of physiological properties were measured. Resting potentials were measured just after the patched membranes were ruptured by suction. Input resistances and time constants of cells were determined by passing hyperpolarizing current pulses (duration, 500–600 msec) inducing voltage shifts of 6–15 mV negative to rest. Time constants were measured by fitting to a single exponential. Spike threshold and spike widths at half amplitude were measured for spikes elicited by depolarizing current pulses (duration, 50 msec) of threshold strength. It was investigated by depolarizing current pulses (duration, 500–600 msec) of threshold strength from −75 to −85 mV whether cells could generate low-threshold spikes or not. Membrane potentials have been corrected for junction potentials (+5 mV) for off-line analyses.

*Histological methods.* Most slices containing biocytin-filled cells were fixed by immersion in 4% paraformaldehyde and 0.2% picric acid in 0.1 M phosphate buffer (PB) for 1–2 hr at room temperature, followed by incubation in PB containing 5% sucrose and 0.5% Triton X-100 (TX) for 30 min. The tissue was next frozen with dry ice, then thawed in PB to make chemical agents penetrate deeper into the slices. The slices were incubated in PB containing 0.5% $H_2O_2$ for 30 min to suppress endogenous peroxidase activity. They were then incubated for 4–6 hr at room temperature in Tris-buffered saline (TBS) containing an avidin-biotin-peroxidase complex (ABC solution, Vector) at a dilution of 1:200 and 0.5% TX. The slices were reacted with 3,3′-diaminobenzidine tetrahydrochloride (DAB, 0.05%) and $H_2O_2$ (0.003%) in PB, followed by incubation in 0.1% osmium tetroxide in PB for 5 min. After dehydration, the slices were mounted, embedded in Epon 812 (Fluka), and coverslipped.

After fixation and freeze-and-thaw procedure, some slices were incubated for 4–6 hr in TBS containing streptavidin-conjugated fluorescein isothiocyanate (FITC) (Vector; diluted 1:200) and imaged with a confocal microscope (Bio-Rad, MRC 600). After collecting the fluorescence images, the slices were again processed to make biocytin staining more permanent. They were incubated in TBS containing 0.5% $H_2O_2$, followed by incubation with biotin–peroxidase (Vector; diluted 1:200) in TBS for 3 hr. They were then incubated for 3 hr in TBS containing avidin-biotin-peroxidase complex (diluted 1:200). The slices were reacted with DAB, osmificated, and embedded as above.

The dendrites, axonal processes, and somata of labeled neurons were drawn using a camera lucida. Data are given as mean ± SD. For statistical analysis in comparing cell classes, the Mann–Whitney $U$ test was used.

*Immunohistochemical procedure for immersion-fixed slices.* For immunohistochemical identification of recorded cells, whole-cell recording was terminated and the slices put into the fixative within 5 min after breaking the patched membrane in order to lower the possibility of reducing the somatic concentration of parvalbumin by dilution of intracellular fluid with the pipette solution. Slices containing biocytin-loaded cells were fixed by immersion in 4% paraformaldehyde and 0.2% picric acid in PB for 1 hr at room temperature, and incubated in PB containing 5% sucrose and 0.5% TX for 30 min. The tissue was frozen with dry ice and thawed in PB. The slices were again incubated in PB containing 0.5% TX, frozen with dry ice, and thawed in PB to make antibodies penetrate deeper into the slices. The slices were then incubated overnight at room temperature with a mouse monoclonal antibody against parvalbumin (Sigma; diluted 1:2000) in TBS containing 10% normal goat serum (NGS), 2% bovine serum albumin (BSA), and 0.5% TX, followed by incubation for 3 hr in a mixture of streptavidin-conjugated 7-amino-4-methylcoumarin-3-acetic acid (AMCA) (Vector; diluted 1:400) and tetramethylrhodamine isothiocyanate (TRITC)-conjugated goat anti-mouse IgG (Chemicon; 1:200), dissolved in TBS containing 10% NGS, 2% BSA. This procedure allowed observations in double fluorescence of AMCA-labeled biocytin and TRITC-labeled parvalbumin. The sections were observed and photographed in a fluorescence microscope (Nikon Microphot-FXA) using the G-2A (Nikon) filter block for TRITC and XF03 (Omega Optical) block for AMCA. In addition, a bandpass filter (400–500 nm, BPB-45 FUJI) was used for AMCA.

*Immunohistochemistry in perfusion-fixed brains.* Two male Wistar rats (20 d postnatal) were used. The animals were given an overdose of Nembutal and perfused through the heart with a solution (10 ml) consisting of 160 mM sucrose and 0.1% paraformaldehyde in PB, followed by 150 ml of fixative containing 2% paraformaldehyde, 0.2% picric acid, and 0.1% glutaraldehyde in PB. The brains were removed and postfixed in the same fixative for 3 hr at 4°C. After incubation in PB containing 30% sucrose for 3 d at 4°C, cryostat sections were cut along the line of the rhinal fissure at 10 μm and mounted on silane-coated slides. The sections were incubated overnight at room temperature with a monoclonal mouse antibody against parvalbumin (diluted 1:2000) and a rabbit antiserum against GABA (Sigma; diluted 1:4000) in TBS containing 10% NGS, 2% BSA, and 0.5% TX, followed by incubation for 3 hr in dichlorotriazinyl-aminofluorescence-dihydrochloride (DTAF)-conjugated goat anti-mouse IgG (Chemicon, 1:200) for parvalbumin and TRITC-conjugated donkey anti-rabbit IgG (Chemicon, 1:200) for GABA, in TBS containing 10% NGS, 2% BSA. This procedure allowed immunofluorescence observations for parvalbumin and GABA. The sections were observed in a fluorescence microscope using the G-2A (Nikon) dichroic mirror system for TRITC and B-2E (Nikon) for DTAF.

## Results

Neurons were sampled by whole-cell recording from layer II/III and at the border between layers II/III and V of frontal agranular cortex, and only cells with resting potentials more negative than −51 mV and overshooting spikes were selected for analysis. Staining intracellularly with biocytin clearly distinguished the morphologies of nonpyramidal cells (Fig. 1) and pyramidal cells. In no cases were two or more cells stained by a single whole-cell recording. Pyramidal cells had apical and basal dendrites with many spines and main axons that always went straight toward the white matter. Nonpyramidal cells lacked apical dendrites and the dendrites either lacked spines or had less spines than pyramidal cells. All electrophysiological data used for the analysis came from morphologically identified nonpyramidal cells, whose local axons were stained enough to classify the cells morphologically according to the branching and distribution patterns of their axons.

Eighty-four layer II/III nonpyramidal cells which satisfied the above electrophysiological and morphological criteria were divided into four physiological classes (Table 1). Fast-spiking cells (FS cells, $n$ = 29) fired trains of action potentials of shorter

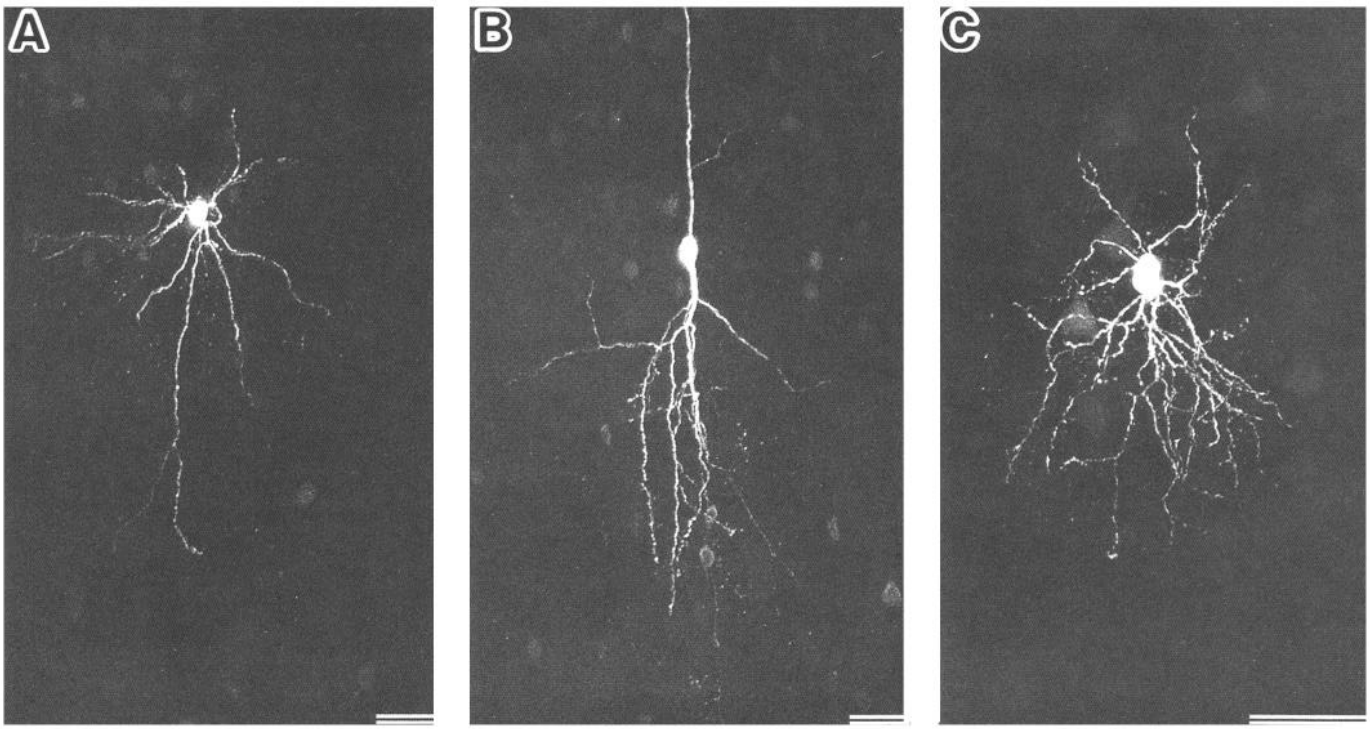


*Figure 1.* Photomicrographs of three layer II/III nonpyramidal cells intracellularly stained by biocytin. The cells were visualized by streptavidin-conjugated FITC and observed by confocal microscopy. *A*, An FS (fast-spiking) multipolar cell. *B*, An RSNP (regular-spiking nonpyramidal cells) bipolar cell. *C*, An LS (late-spiking) neurogliaform cell. Scale bar, 50 μm.

**Table 1. Properties of four subgroups of layer II/III nonpyramidal cells**

| | FS cells ($n$ = 29) | LS cells ($n$ = 9) | LTS cells ($n$ = 4) | RSNP cells ($n$ = 41) |
|---|---|---|---|---|
| Soma diameter (μm) | 15.7 ± 2.7 [12.7–24.0] (<RSNP) | 13.6 ± 1.2 [12.2–15.4] (<RSNP) | 15.2 ± 1.7 [12.7–16.7] | 16.2 ± 2.8 [10.4–23.0] (>LS) |
| Resting potential (mV) | −77.4 ± 2.9 [−85–−72] (≪) | −67.2 ± 5.5 [−78–−59] (>FS,<RSNP) | −57.5 ± 7.4 [−68–−51] (>FS) | −60.6 ± 5.1 [−74–−51] (>FS,LS) |
| Input resistance[a] (MΩ) | 157 ± 42 [74–256] (≪) | 297 ± 118 [124–543] (>FS) | 460 ± 144 [288 ± 594] (>FS) | 414 ± 207 [188–1132] (>FS) |
| Time constant[a] (msec) | 8.8 ± 2.0 [5.2–14.1] (≪) | 20.6 ± 8.0 [8.1–37.0] (>FS) | 54.7 ± 26.4 [30.5–89.8] (>FS) | 28.5 ± 12.2 [11.8–62.6] (>FS) |
| Spike threshold (mV) | −41 ± 5 [−50–−32] (>RSNP) | −38 ± 4 [−44–−33] (>RSNP) | −46 ± 3 [−49–−43] | −45 ± 4 [−53–−39] (<FS,LS) |
| Spike width[b] (msec) | 0.43 ± 0.06 [0.33–0.58] (≪) | 0.77 ± 0.19 [0.57–1.05] (>FS) | 0.94 ± 0.15 [0.79–1.14] (>FS) | 0.75 ± 0.13 [0.48–1.12] (>FS) |

Data are mean ± SD; numbers in parentheses are ranges. FS cells, fast-spiking cells: LS cells, late-spiking cells; LTS cells, low-threshold spike cells; RSNP cells, regular-spiking nonpyramidal cells. >*A*, <*B*, significantly larger than that of *A* cells and smaller than that of *B* cells, respectively ($p \leq 0.005$); ≪, significantly smaller than that of the other types of cells ($p \leq 0.005$).

[a] Input resistance and time constant were determined by hyperpolarizing current pulses inducing voltage shift of 6–15 mV negative to rest.

[b] At half-amplitude.

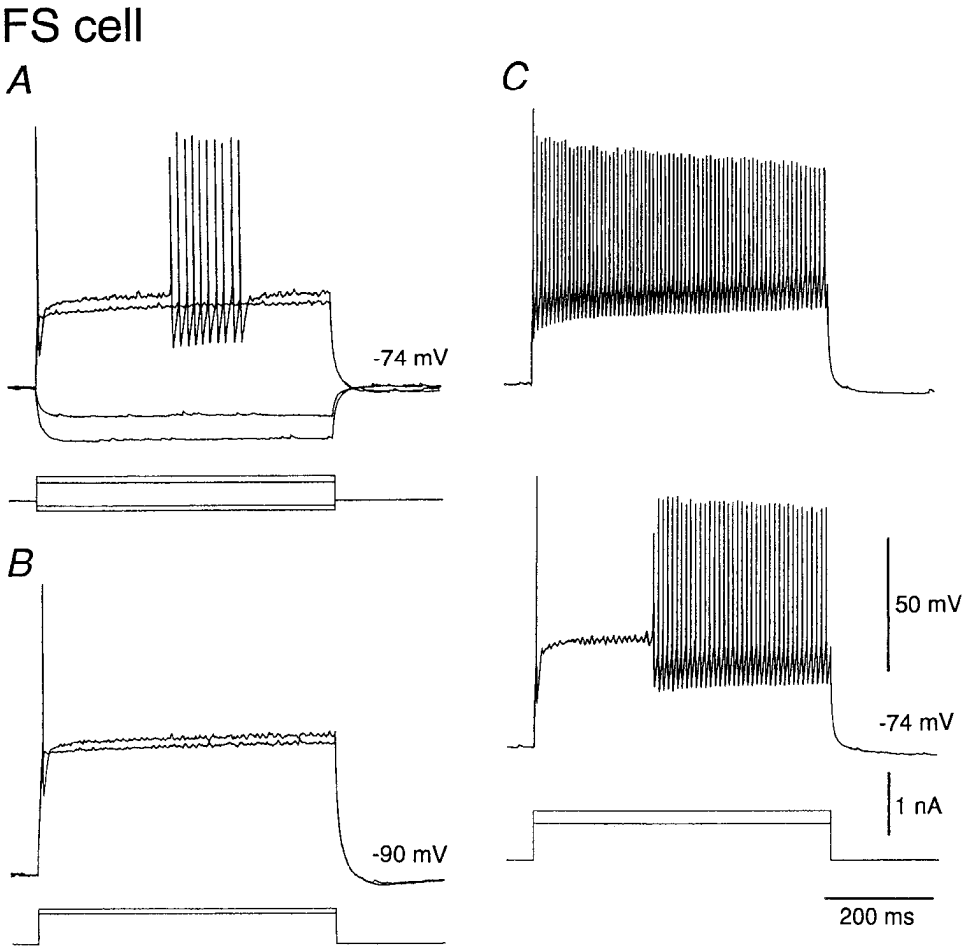


*Figure 2.* Physiological characteristics of an FS (fast-spiking) nonpyramidal cell. *A,* Voltage responses induced by current pulses and repetitive spike discharges induced by a current pulse close to the threshold. Note short afterhyperpolarization following a spike. A depolarizing pulse induced early single firing and late repetitive firing. Note abrupt start and cessation of firing. Spikes are truncated due to sampling frequency. *B,* No low-threshold spikes were elicited by depolarizing pulses from hyperpolarized potentials. *C,* Two firing responses by depolarizing pulses. Note abrupt start of repetitive firing and weak adaptation of firing rate during repetitive discharges. Membrane potentials are written on each record. Resting membrane potential, −74 mV.

duration at constant frequency. Late-spiking cells (LS cells, $n$ = 9) exhibited slowly developing ramp depolarizations before firing spikes. Low-threshold spike cells (LTS cells, $n$ = 4) fired prominent low-threshold spikes from hyperpolarized potentials. Regular-spiking nonpyramidal cells (RSNP cells, $n$ = 41) did not show fast-spiking characteristics, low-threshold spikes, or ramp depolarizations. Nonpyramidal cells not categorized into one of the above three subgroups were classified as RSNP cells. These four physiological subgroups also had different morphological characteristics. Although morphological data, particularly the full extent of dendrites and axons, were limited by slice thickness, each class of nonpyramidal cells showed characteristic branching patterns of dendrites and axons (Jones, 1975; Feldman and Peters, 1978; Fairén et al., 1984; Lund and Lewis, 1993). The detailed description of electrophysiological properties and morphological characteristics of each class of nonpyramidal cells follows.

*Fast-spiking nonpyramidal cells (FS cells)*

Among 84 identified nonpyramidal cells, 29 cells (35% of the total sample) belonged to the FS class. A characteristic property of FS cells was a constant rate of spikes during an episode of repetitive firing. At near-threshold current levels, discharges consisted of either single spike at the beginning of the current pulse, or a variable-duration episode of repetitive discharge after a quiescent period, or both (Fig. 2). Stronger current stimuli elicited constant-rate repetitive firing throughout the current pulses (Fig. 2*C*). The frequencies of spike discharge during an episode of repetitive discharges were quite constant even at high discharge rate (Fig. 2). Another feature of FS cells was their shorter-duration action potentials, followed by fast afterhyperpolarizations (Table 1). FS cells had lower input resistances in comparison with other classes of cells, as well as resting membrane potentials more negative than those of the other types of nonpyramidal cells (Table 1).

FS cells were mostly multipolar and had smooth dendrites (Figs. 1*A*, 3). The dendrites of FS cells distributed in layer II/III, in layers I and II/III, or in layers II/III and V. The axons of FS cells originated from the somata or the dendrites. The axonal innervations were mainly in layer II/III, but, in some cells, also in layer V. The axon collaterals of FS cells never entered layer I. FS cells could be divided into two morphological subtypes according to their axonal innervation patterns.

*FS cells with local axonal arbors and horizontal axonal arbors.* Among 29 FS cells, 26 cells were classified into this subtype. This type of FS cell innervated densely the region near the soma by fine branches, and the axon collaterals ran in nonpreferential directions (Fig. 3*A*). Some cells also had collaterals, running in a horizontal direction along layer II/III, 500–800 μm in width (Fig. 3*B*). Many cells of this type also had a few axonal branches descending into layer V. The width of the dendritic field was 250–350 μm. It was observed by interference microscopy that some axonal boutons of this type surrounded somata of other cells (Kawaguchi and Kubota, 1993). From these patterns of axonal arbors and boutons, this

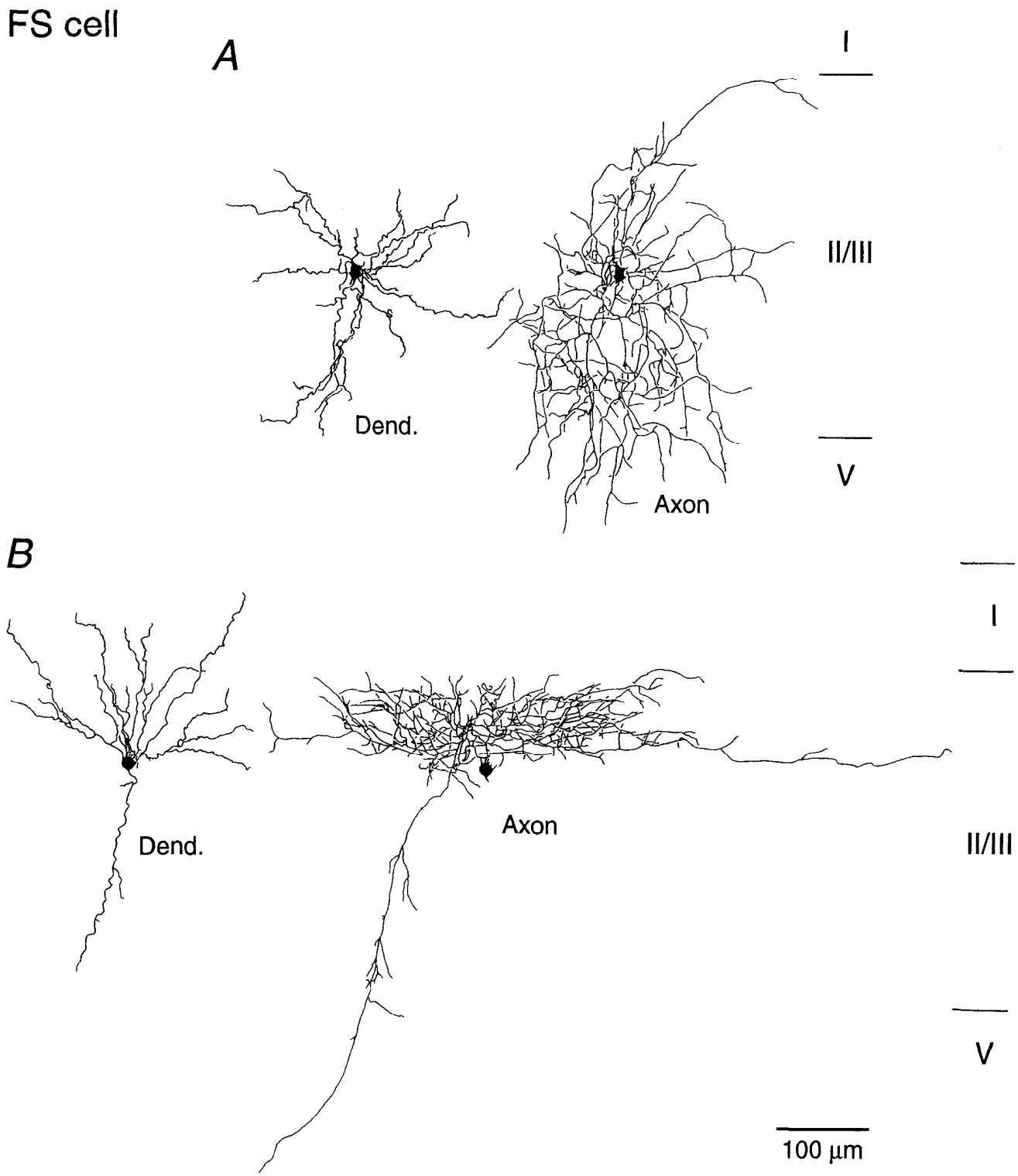


*Figure 3.* Reconstructions of FS cells. *A*, An FS cell with local axonal arbors. Note that the axonal arborizations are similar to the dendritic field in width. *B*, An FS cell with local and horizontal axonal arbors. Note most axonal branches are confined to upper layer II/III and do not enter layer I.

class was considered to contain some basket cells (Fairén et al., 1984).

*FS chandelier cells.* Four chandelier cells were recorded in this study (Figs. 4, 5). The axonal branches showed axon "cartridges" with boutons characteristic of chandelier cells (Somogyi, 1977; Peters, 1984a). Three were identified as FS cells. The dendrites of these three cells extended into layer I (Fig. 4). The axonal innervations were mainly in the superficial part of layer II/III.

Out of four chandelier cells, one cell could not be identified

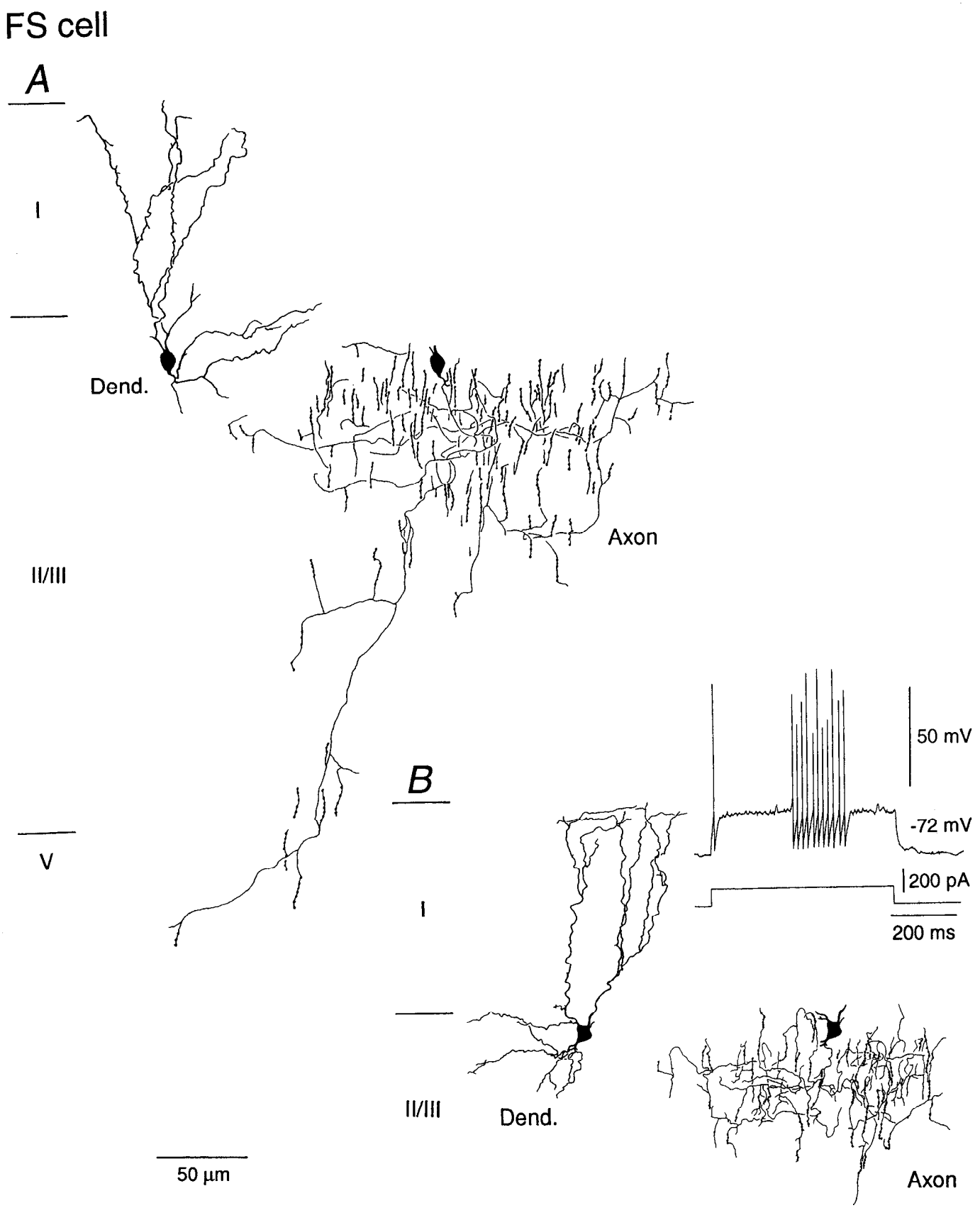


*Figure 4.* *A* and *B*, FS chandelier cells. Both cells situate in upper layer II/III and most of the dendrites are in layer I. Note the characteristic vertically oriented candles of axonal boutons. *B: Inset,* A firing response of this chandelier cell by a depolarizing pulse. Note abrupt repetitive spike discharges with weak adaptation of firing rate characteristic of FS cells.

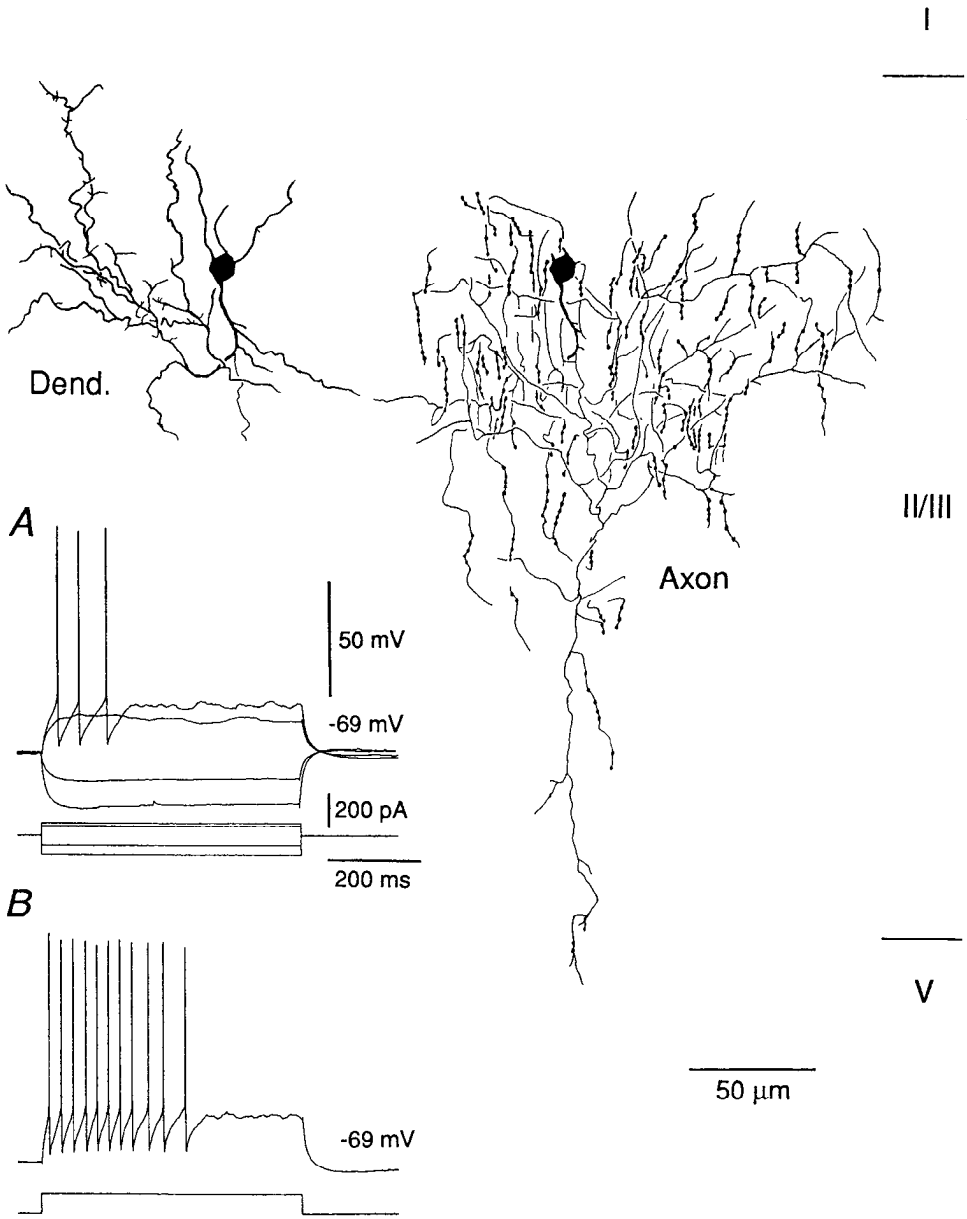


*Figure 5.* A chandelier cell which did not show abrupt nonadapting repetitive spike discharges and could not be identified physiologically. The dendrites are mainly in layer II/III. *A: Inset,* Voltage responses and spike discharges induced by current pulses. *B,* Repetitive spike discharges showed spike-frequency adaptation. Membrane potentials are written on each record. Resting membrane potential, −69 mV.

as an FS cell (Fig. 5). This chandelier did not show abrupt nonadapting repetitive spike discharges and the spike width at half amplitude was 0.64 msec. The dendrites were almost smooth and only in layer II/III in contrast to the above three FS cells. The axonal innervations were mainly in the upper part of layer II/III.

*Late-spiking nonpyramidal cells (LS cells) (LS neurogliaform cells)*

Among 84 identified nonpyramidal cells, nine cells belonged to the LS class (11% of the total sample). A characteristic membrane property of LS cells was a slowly developing ramp depolarization when depolarized by current pulses near threshold (Fig. 6*A*). In response to threshold current pulses, membrane potentials did not reach steady state and finally triggered action potentials. The ramp depolarizations of LS cells could be induced from both depolarized and hyperpolarized states (Fig. 6*B*). Threshold depolarizing current pulses could not produce low-threshold spikes from hyperpolarized potentials (Fig. 6*B*). When stimulated by current pulses just above threshold, LS cells fired repetitively at constant rates (Fig. 6*C*) and did not adapt. In response to current pulses at 2× threshold, LS cells showed slight spike-frequency adaptation (Fig. 6*C*). LS cells had wider spikes, higher input resistances, and more positive resting membrane potentials than those of FS cells; resting potentials were more negative than those of RSNP cells (Table 1).

LS cells were multipolar (Figs. 1*C*, 6*D*) and had smaller cell bodies (Table 1). Their dendrites were smooth and distributed in layer II/III or in layers I and II/III. The width of the dendritic field was 100–200 μm, and the dendrites made a symmetrical, spherical field. The axons, originating from the somata and the dendrites, immediately branched and rebranched frequently, creating an entangled plexus. The axonal innervations were mainly in layer II/III, but, in some cells, also extended into layer I or layer V. The width of the axonal arbor was 250–300 μm, which was twice as wide as that of the dendritic field. From these morphological characteristics, these LS cells are considered to be neurogliaform cells (Jones, 1984).

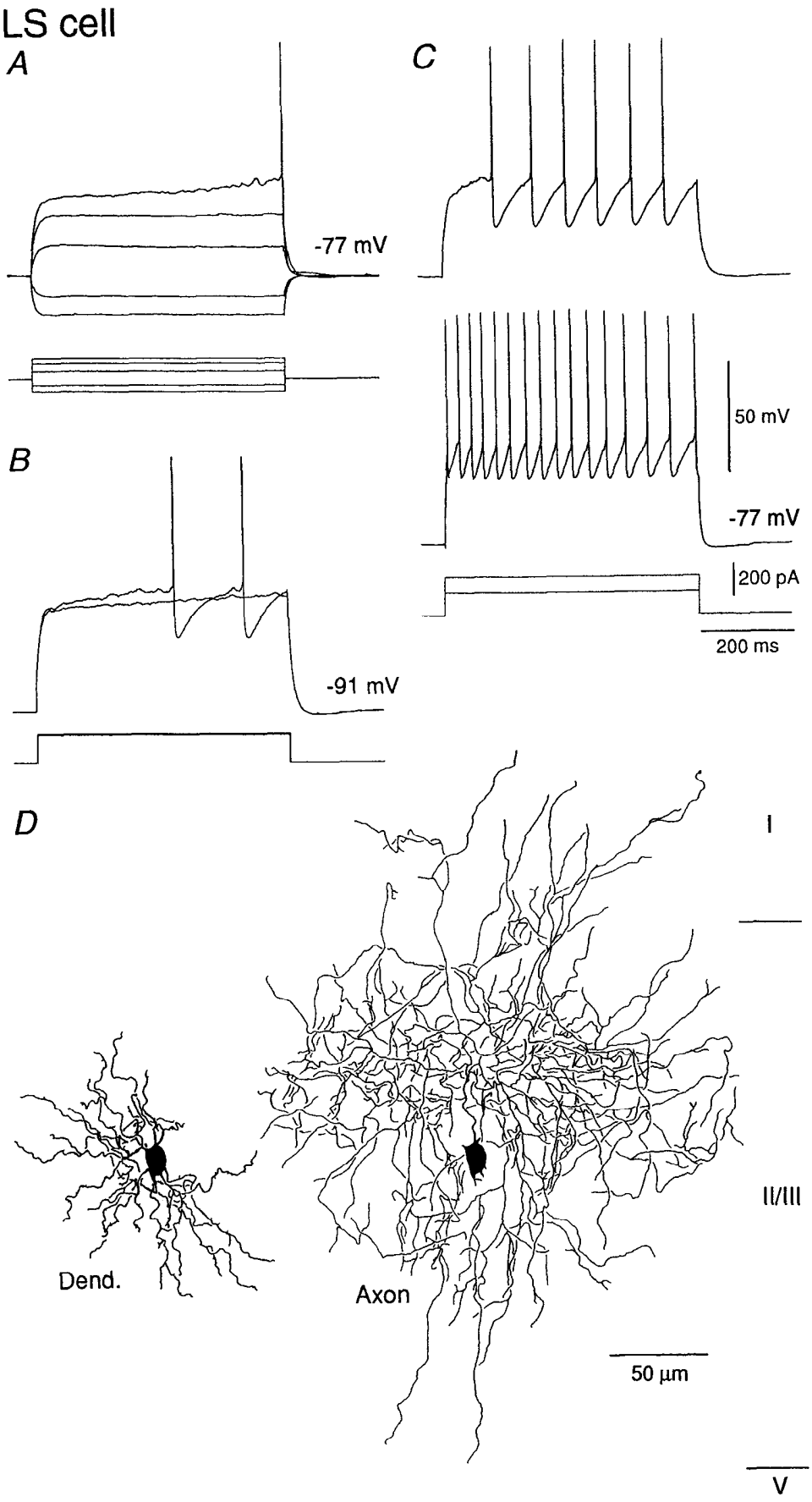


*Figure 6.* Physiological and morphological characteristics of LS (late-spiking) nonpyramidal cells. *A,* Voltage responses induced by current pulses and a spike discharge induced by current pulse close to the threshold. Note the slowly developing ramp depolarization before a spike firing. *B,* No low-threshold spikes were elicited by depolarizing pulses from hyperpolarized potentials. Slowly developing ramp depolarizations could be also elicited from hyperpolarized potentials. *C,* Two firing responses by depolarizing pulses. Note the relatively constant firing rate during repetitive firing at lower rate of discharges. Membrane potentials are written on each record. Resting membrane potential, −77 mV. *D,* An LS (late-spiking) neurogliaform cell. Note the narrow dendritic field and the restricted horizontal spread of the axonal collaterals.

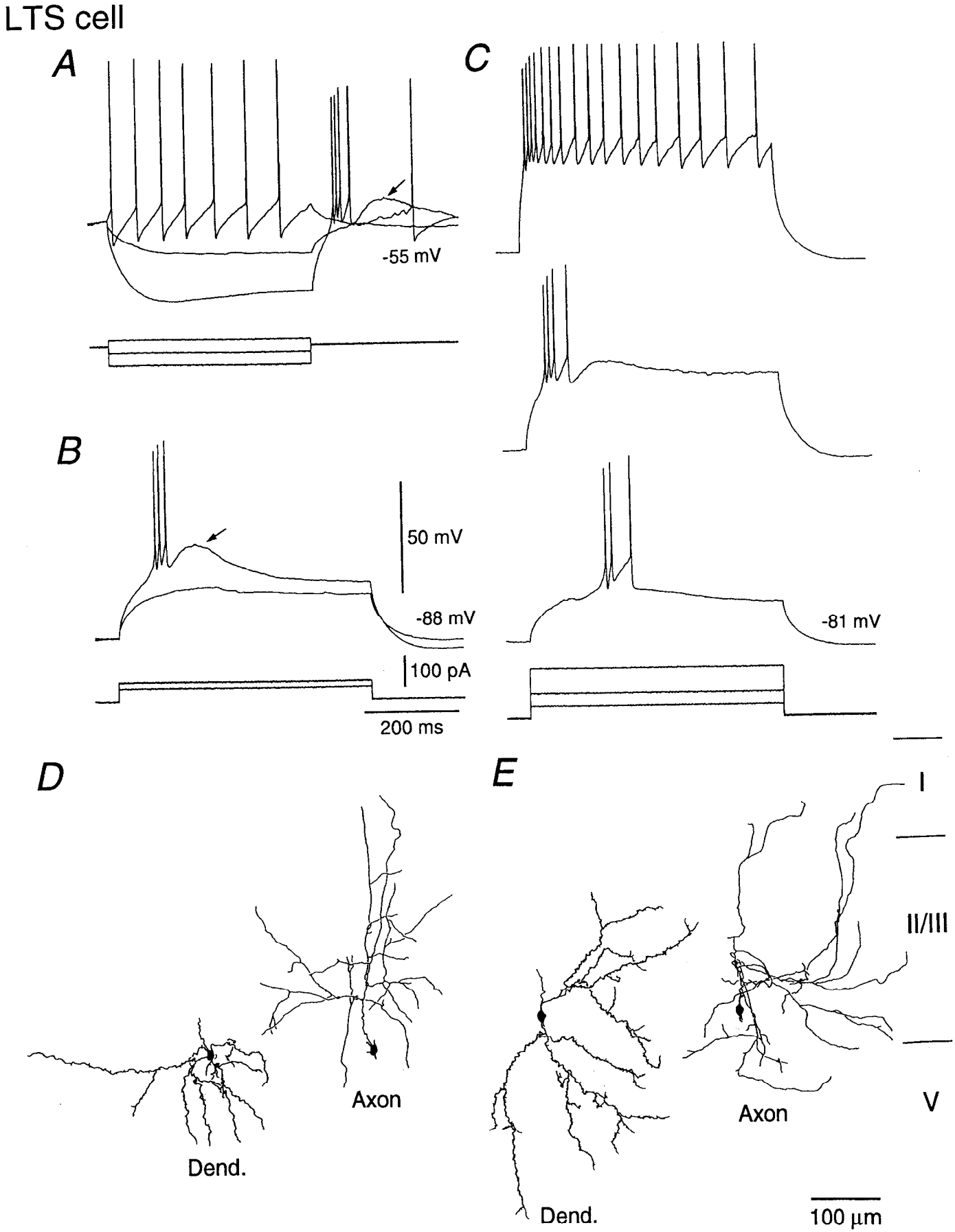
LTS cell
A
-55 mV
B
50 mV
-88 mV
100 pA
200 ms
C
-81 mV
D
Axon
Dend.
E
I
II/III
V
Axon
Dend.
100 µm

*Low-threshold spike nonpyramidal cells (LTS cells) (LTS cells with ascending axons)*

Four cells belonged to this class (5% of the total sample). These cells were comparable to layer V LTS cells (Kawaguchi, 1993), but were encountered much less frequently in layer II/III. LTS cells were distinguished from other classes of cells by their ability to fire prominent low-threshold spikes (Fig. 7). Low-threshold spikes could be induced by depolarizing pulses only at holding potentials more negative than about −70 to −80 mV (Fig. 7*B*). Low-threshold spikes were also elicited by cessation of hyperpolarizing pulses at depolarized potentials (Fig. 7*A*). Duration of low-threshold spikes ranged from 153 to 282 msec (mean = 189 msec, SD = 62 msec). LTS cells usually could generate 2–4 regular spikes riding on each low-threshold spike. Spike-frequency adaptation of LTS cells during depolarizing pulses was prominent in spike trains following low-threshold spikes (Fig. 7*C*). Spike-frequency adaptation was also observed in spike trains without low-threshold spikes (Kawaguchi, 1993). LTS cells had longer spike width, higher input resistances, and more positive resting membrane potentials than those of FS cells (Table 1).

LTS cells had multipolar or bitufted dendritic patterns, and had dendrites with a modest number of spines (Fig. 7*D,E*). Among the four cells of this type, two were in layer II/III and the other two at the border area between layers II/III and V. The dendrites of the cells in layer II/III extended in layer II/III or in layers II/III and V (Fig. 7*E*). The cells at the border area had dendrites mainly in layer V (Fig. 7*D*). The width of the dendritic field was 300–400 μm. The axons originated from the pia side of the soma or from the dendrites at the pia side. The main axons ascended and the collaterals entered into layer I and also distributed in layers II/III and V. The width of the axonal arbor was 300–500 μm.

*Regular-spiking nonpyramidal cells (RSNP cells) (RSNP cells with vertical axonal arbors)*

Nonpyramidal cells not categorized into one of the above three subgroups were placed in the RSNP subgroup. Among 84 identified nonpyramidal cells, 41 cells (49%) belonged to this class. This class of nonpyramidal cells did not show easily defined electrophysiological properties, but they were nonpyramidal in shape (Fig. 8; see Fig. 10). At threshold stimuli levels, RSNP cells fired regular spikes at early parts of the current pulses without prominent slow depolarizations (see Fig. 10*A*). Stronger depolarizing current pulses induced repetitive firing, but the discharges gradually adapted and often ceased before the end of the current pulse (Fig. 8; see Fig. 10). Stronger hyperpolarizing current pulses often elicited sag which was characterized as a decay of the voltage response (see Fig. 10*A*, arrow). Threshold current pulses for spike initiation could not generate prominent low-threshold spikes from hyperpolarized potentials (see Fig. 10*B*). Among 41 RSNP cells, 19 cells exhibited a fast depolarizing "notch" following a spike when depolarized from hyperpolarized potentials (Fig. 8*B*, arrow) or upon cessation of hyperpolarization (Fig. 8*A*, arrow). The duration of these fast notches ranged from 30 to 76 msec (mean = 55 msec, SD = 14 msec, $n$ = 19), much shorter than low-threshold spikes of LTS cells (see Fig. 7). RSNP cells had longer spike widths and were higher in input resistances than FS cells; RSNP cells had more positive resting membrane potentials than FS and LS cells (Table 1).

Among 19 RSNP cells with fast depolarizing notches, 10 cells were multipolar (Fig. 9*A*), and the other nine were bipolar or bitufted (Figs. 8*C*, 9*B*). The dendrites were sparsely spiny. It was difficult to distinguish bipolar from bitufted dendritic morphologies. Some cells had two principal dendrites emerging from the upper and lower poles of the somata, and one of the two principal dendrites extended relatively straight toward the pia or the white matter (Figs. 1*B*, 8*C*); these cells were considered to be typical bipolar cells (Feldman and Peters, 1978). Some cells were considered to be bitufted cells rather than bipolar cells (Fig. 9*B*). The dendrites of multipolar cells distributed mainly in layers I and II/III, and those of bipolar (bitufted) cells from layer I to V. The widths of the dendritic fields of this type were 150–300 μm. The common characteristic among these cells was their vertically elongated axonal fields extending from layer I to V, sometimes to layer VI (Figs. 8*C*, 9). The axons originated from the somata or the dendrites. The widths of the axonal arbor of multipolar and bipolar (bitufted) cells of this type were 200–500 μm and 150–300 μm, respectively.

The remaining RSNP cells ($n$ = 22), in which fast depolarizing notches could not be detected, also extended axonal branches vertically from layer I to upper layer V (Figs. 10*C*, 11). This type contained both multipolar and bitufted cells. Four cells had the somata at the border between layers II/III and V (Fig. 11*A*). They had axons ascending up to layer I. The dendrites of this type were restricted in layer V in three cells and in both layers II/III and V in one cell, and were sparsely or modestly spiny. The somata of the other 13 cells were in layer II/III. The axons of this type had mainly ascending branches up to layer I and also some branches into layer V (Figs. 10*C*, 11*B,C*). The axons originated from the somata or the dendrites. The widths of the axonal arbors of this type were 150–550 μm, but the axons could be traced more than 1 mm horizontally in one case (Fig. 11*C*). The widths of the dendritic fields were 100–400 μm.

Because both bitufted cells with vertically oriented axonal arbors (double bouquet cells; Somogyi and Cowey, 1984) (Figs. 9*B*, 10*C*) and cells with vertically elongated axonal plexus and dendritic tree formed by principal dendrites (bipolar cells; Peters, 1984b) (Figs. 1*B*, 8*C*) were found in RSNP cell, double bouquet cells and bipolar cells are considered to belong to RSNP cells.

←

*Figure 7.* Physiological and morphological characteristics of LTS (low-threshold spike) nonpyramidal cells. *A*, Voltage responses and spike discharges induced by current pulses. Note that an all-or-none low-threshold spike (*arrow*) with regular spikes was induced by cessation of hyperpolarizing pulses at resting potentials. *B*, A low-threshold spike (*arrow*) was also elicited by a depolarizing pulse from hyperpolarized potentials. *C*, Three firing responses by depolarizing pulses from hyperpolarized potentials. Note the threshold differences between low-threshold spikes with regular spikes (*middle* and *lower traces*) and repetitive discharges of regular spikes (*upper trace*). Note the spike-frequency adaptation during repetitive discharges (*upper trace*). Membrane potentials are written on each record. Resting membrane potential, −55 mV. *D*, This cell has the soma at the border between layer II/III and V. Most of the dendrites are within layer V. Note that the axonal branches go up to layer I. *E*, This cell has a bitufted shape and the soma in layer II/III. The dendrites are extended in both layer II/III and V. Note the axonal branches going upward.

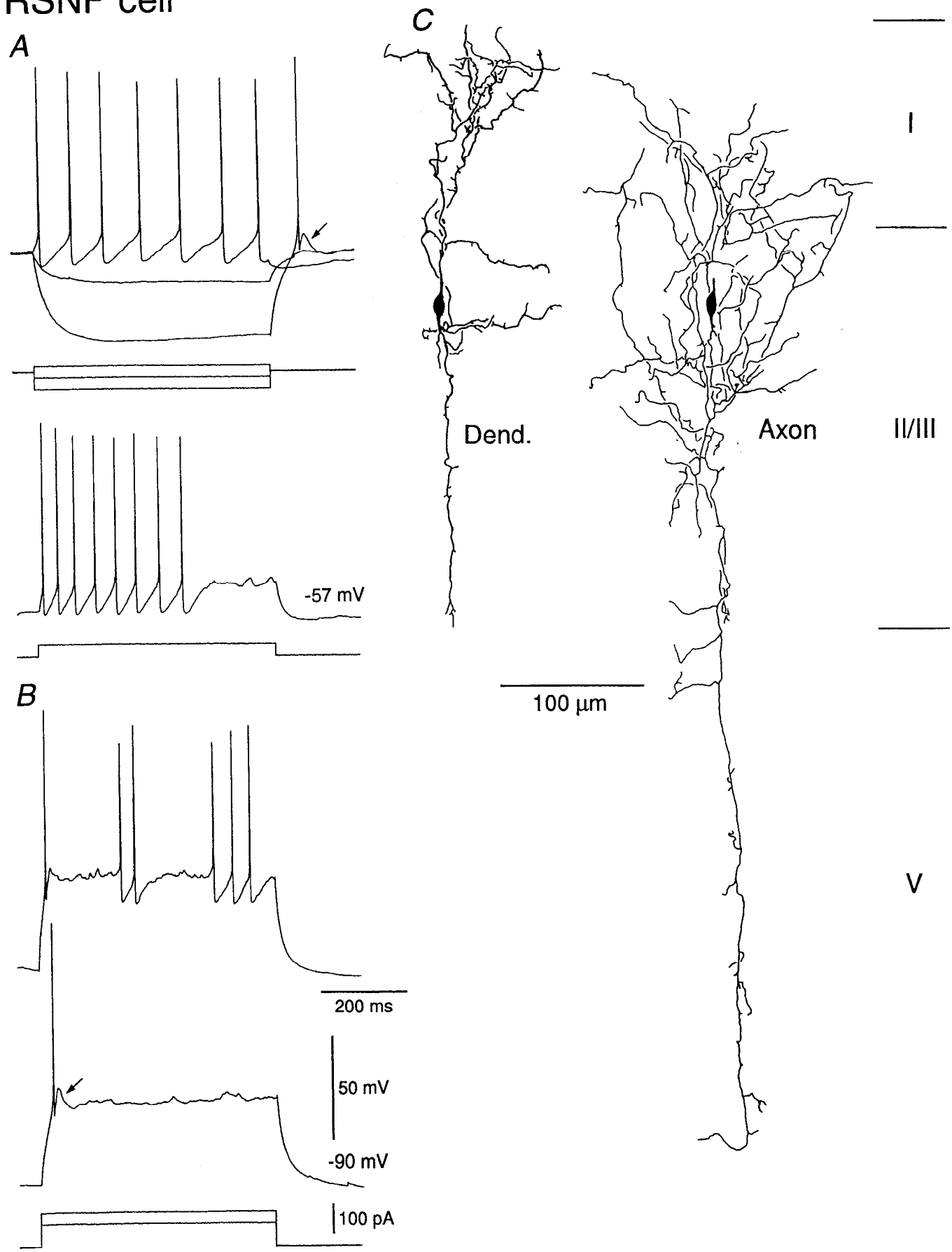
RSNP cell
A
-57 mV
B
200 ms
50 mV
-90 mV
100 pA
C
Dend.
Axon
100 µm
I
II/III
V

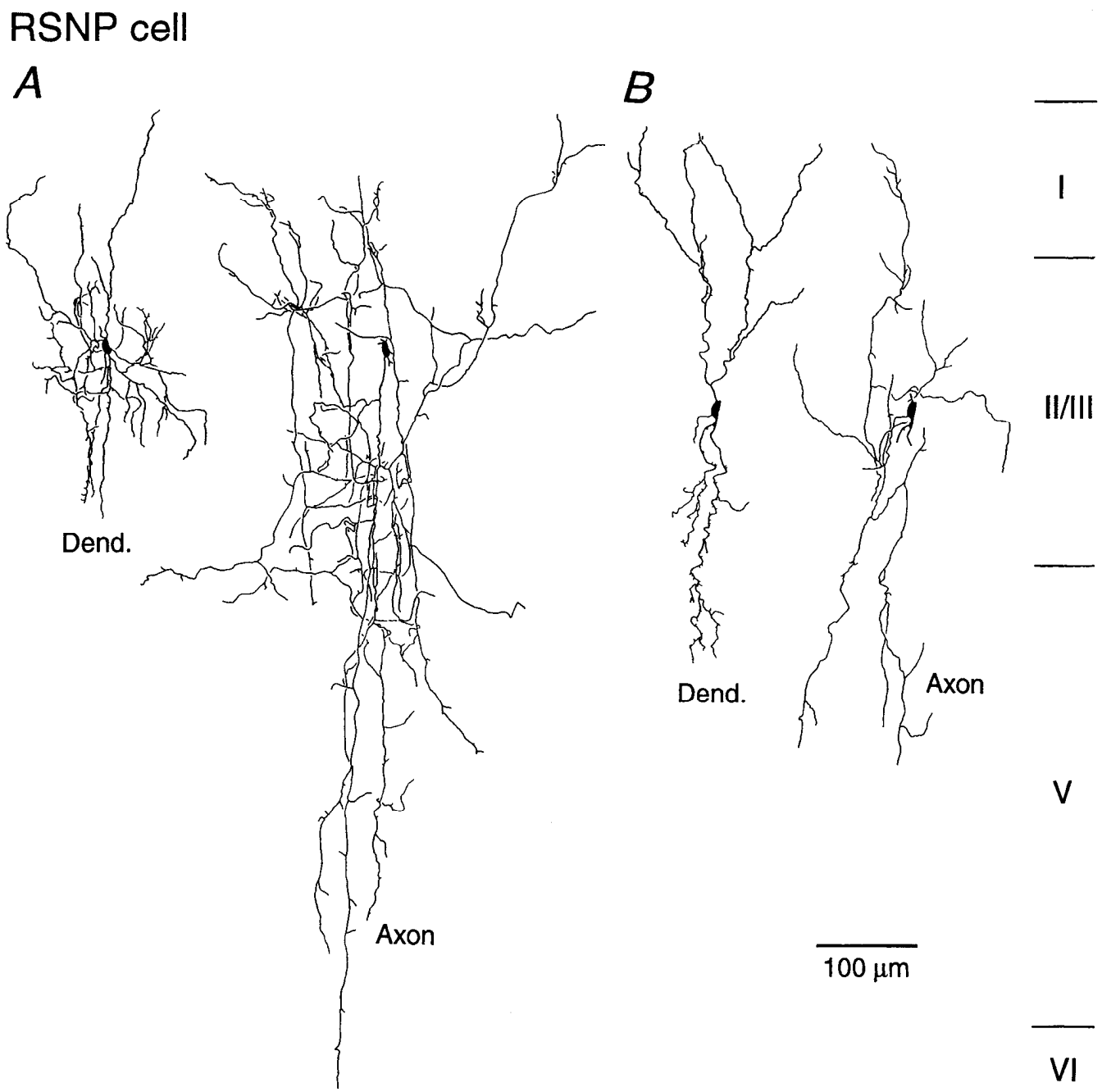


*Figure 9.* Reconstructions of RSNP cells with fast depolarizing notches. They had long vertical axonal arbors. *A,* A multipolar cell. The dendrites are in layer I and layer II/III. The axonal branches are vertically elongated through layer I to VI. *B,* A bitufted cell. The dendrites are through layers I and V.

←

*Figure 8.* Physiological and morphological characteristics of RSNP cells with fast depolarizing notches. *A,* Voltage responses and spike discharges induced by current pulses. *Upper trace,* Note an all-or-none fast depolarizing notch (*arrow*) with a spike was induced by cessation of hyperpolarizing pulses at resting potentials. Note that this depolarizing notch was much shorter in duration than low-threshold spikes in LTS cells. *Lower trace,* In a stronger current pulse, repetitive firing adapted and then ceased. *B,* Two firing responses by depolarizing pulses from hyperpolarized potentials. Note first spike with a depolarizing notch (*arrow*). Membrane potentials are written on each record. Resting membrane potential, −57 mV. *C,* This RSNP cell with depolarizing notches was a bipolar cell. The dendrites are in layer I and layer II/III. Note a vertically elongate and narrow dendritic tree formed by two principal dendrites. Note also vertically oriented axonal branches ascending to layer I and descending to layer V with narrow horizontal spread.

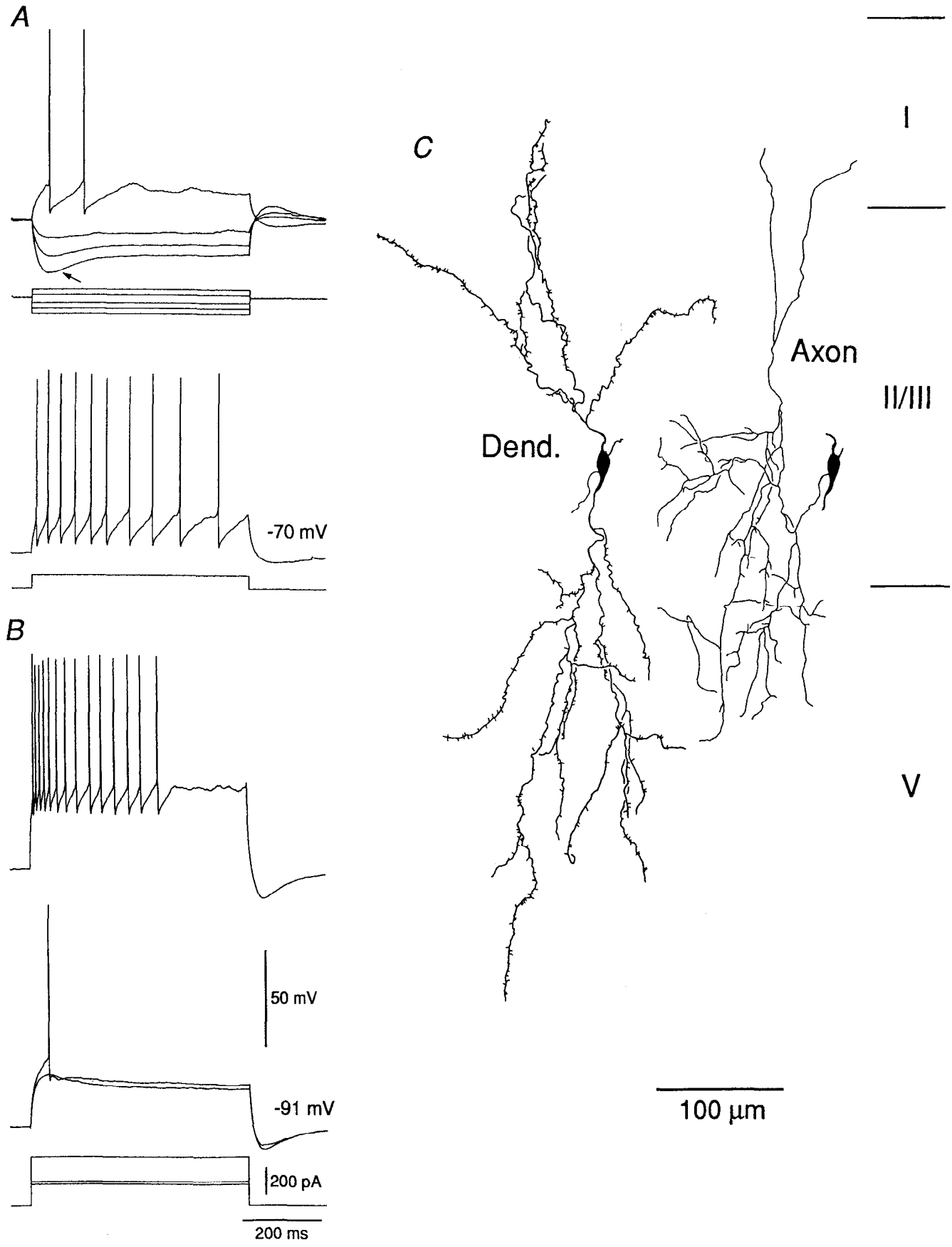
RSNP cell
A
-70 mV
B
50 mV
-91 mV
200 pA
200 ms
C
Axon
Dend.
I
II/III
V
100 µm

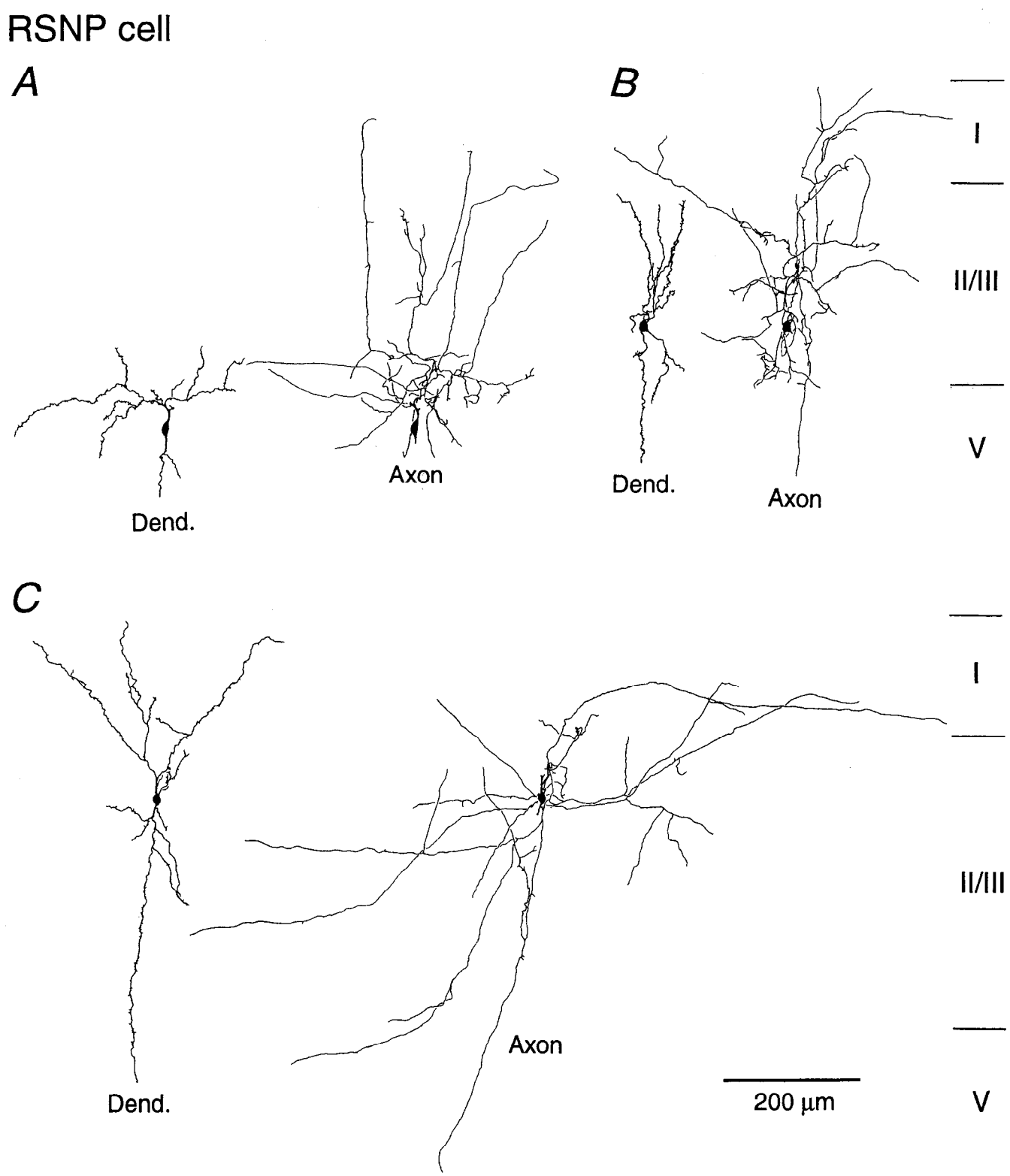


*Figure 11.* Reconstructions of RSNP cells. *A,* A bitufted cell with ascending axons. This has soma at the border between layers II/III and V. Most dendrites are in layer V. Note the axonal branches going up to layer I. *B,* A bitufted cell with vertical axonal arbors. *C,* A bitufted cell with vertical axonal arbors. The dendrites and the axonal branches are elongated through layer I to layer V. Note the wide distribution of axons.
←

*Figure 10.* Physiological and morphological characteristics of RSNP (regular-spiking nonpyramidal) cells. *A: Upper trace,* voltage responses and spike discharges induced by current pulses. A stronger hyperpolarizing current pulse elicited sag (*arrow*); *lower trace,* repetitive spike discharges showed clear spike-frequency adaptation. *B: Lower trace,* low-threshold spikes could not be elicited by depolarizing pulses from hyperpolarized potentials; *upper trace,* a stronger pulse elicited repetitive firing with prominent adaptation and spike trains, then ceased. Note the absence of fast-spiking characteristics, ramp depolarizations, and low-threshold spikes in RSNP cells. Membrane potentials are written on each record. Resting membrane potential, −70 mV. *C,* This RSNP cell had a bitufted shape. Note the axonal branches going up to layer I and also the descending branches into layer V.

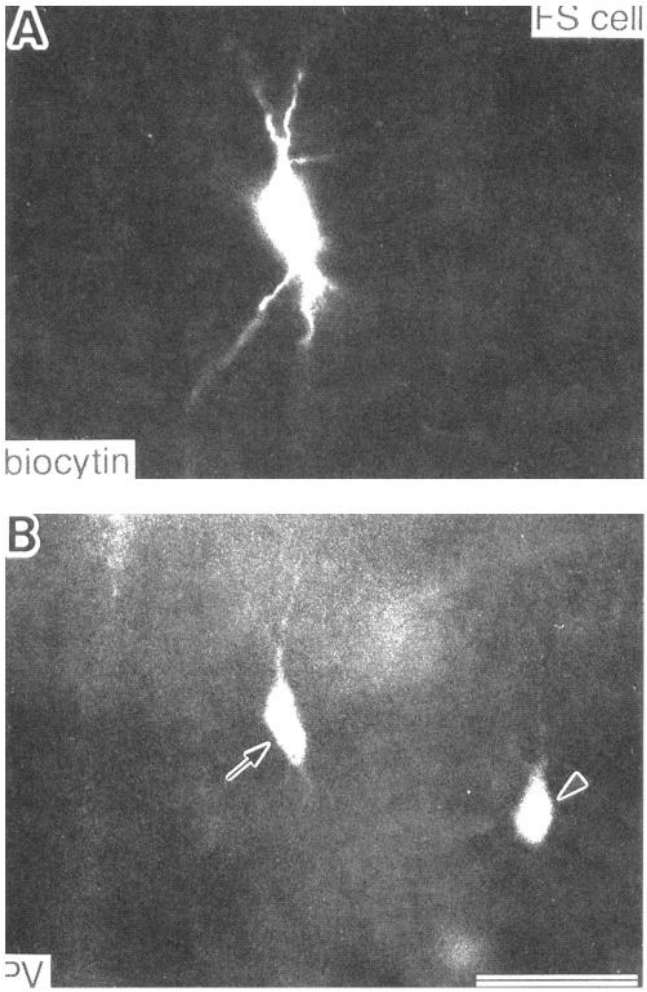


*Figure 12.* Immunohistochemical identification of an FS cell as a parvalbumin-immunoreactive cell. *A*, A biocytin-injected FS cell visualized by AMCA-conjugated avidin. *B*, Parvalbumin (PV) immunoreactivity visualized by TRITC-conjugated secondary antibody in the same section as *A*. *Arrow* indicates the recorded cell. *Arrowhead* indicates another parvalbumin-immunoreactive cell. Scale bar, 50 μm.

### *Identification of recorded FS cells as parvalbumin-immunoreactive cells*

FS cells in layer V of frontal cortex were immunoreactive for parvalbumin, a calcium-binding protein (Kawaguchi and Kubota, 1993). It was investigated by a double fluorescence method whether layer II/III FS cells also showed parvalbumin immunoreactivity. Nonpyramidal cells injected with biocytin were visualized by AMCA-conjugated avidin (blue fluorescence, Fig. 12*A*). Parvalbumin immunoreactivity in the same cells was visualized by a TRITC-conjugated secondary antibody (red fluorescence, Fig. 12*B*). Among 22 layer II/III nonpyramidal cells stained for parvalbumin and identified by physiological subgroup, all FS cells ($n$ = 12) showed immunoreactivity for parvalbumin (Fig. 12). RSNP cells ($n$ = 9), LS cells ($n$ = 3), and LTS cells ($n$ = 1) were not immunoreactive for parvalbumin. The somatic diameter, resting potential, input resistance, time constant, spike threshold, and spike width at half-amplitude of the parvalbumin-positive FS cells were 14.9 ± 3.7 μm, −75.7 ± 2.2 mV, 149 ± 43 MΩ, 9.7 ± 2.3 msec, −41 ± 4 mV, and 0.47 ± 0.07 msec (mean ± SD, $n$ = 12), respectively, which were similar to those of FS cells not identified immunohistochemically (Table 1). Parvalbumin-immunoreactive cells belong to FS cells with local axonal arbors and horizontal axonal arbors. Chandelier cells have not been tested for parvalbumin immunohistochemistry.

The relationship of parvalbumin- and GABA-immunoreactive cells was also investigated in parallel immunohistochemical studies. Double immunocytochemical staining indicated that all parvalbumin-positive cells in layer II/III of medial agranular cortex in 20-d-old rats were immunoreactive for GABA. All 394 parvalbumin-stained cells in layer II/III showed modest to strong staining for GABA. Among 741 GABA-stained cells in layer II/III, 394 cells (53.2%) showed parvalbumin immunoreactivity.

## Discussion

Previously it has been shown that neocortical nonpyramidal cells in layer V of frontal cortex are physiologically heterogeneous (Kawaguchi, 1993) and can be divided into at least two groups with different firing patterns, morphologies, and chemical characteristics (Kawaguchi, 1993; Kawaguchi and Kubota, 1993). However, the results in the present paper indicate that there is a larger variety of physiological subtypes among layer II/III nonpyramidal cells. Four physiological subgroups, also differing in morphological characteristics, were identified in the present study (Fig. 13). (1) FS cells showed an abrupt episode of nonadapting repetitive discharges of shorter-duration action potentials. FS cells had local and horizontal axonal arbors which did not enter layer I. This type of FS cell included some basket cells and parvalbumin-immunoreactive cells which were positive for GABA. Three chandelier cells were FS cells, although one chandelier cell could not be classified as FS cells. (2) LS cells exhibited slowly developing ramp depolarizations near threshold. LS cells were neurogliaform cells. (3) LTS cells had prominent low-threshold spikes from hyperpolarizations. The main axons of LTS cells ascended, and the collaterals entered into layer I. (4) The remaining cells (RSNP cells) could not be categorized into the above three subgroups. Some RSNP cells exhibited fast depolarizing small amplitude notches when depolarized from hyperpolarizations. RSNP cells had vertically elongated axonal fields, extending from layer I to V, sometimes to layer VI. This subgroup included double bouquet cells and bipolar cells.

### *Which subgroups are GABAergic?*

Most nonpyramidal cells in the cortex are supposed to be GABAergic (Houser et al., 1983; Jones, 1993). From the positive staining of some FS cells for parvalbumin, FS cells are considered to be GABAergic because parvalbumin cells are all im-

→

*Figure 13.* Schematic summary of discharge patterns and morphologies of dendrites and axons of four subgroups of nonpyramidal cells. *Traces in rectangles* are intracellular recordings from nonpyramidal cells in response to suprathreshold current pulses. Dendrites and axons are drawn in *black* and *red*, respectively. *A*, FS cell with local axonal arbors. *B*, FS cell with local and horizontal axonal arbors. *C*, FS chandelier cell. *D*, LS neurogliaform cell. *E*, LTS multipolar cell with ascending axons. *F*, LTS bitufted cell with ascending axons. *G*, RSNP multipolar cell with vertical axonal arbors. *H*, RSNP bitufted cell with vertical axonal arbors (double bouquet cell). *I*, RSNP bipolar cell with vertical axonal arbors. *J*, RSNP cell with ascending axons. *K*, RSNP bitufted cell with vertical axonal arbors (double bouquet cell). *L*, RSNP bitufted cell with wide axonal arbors.

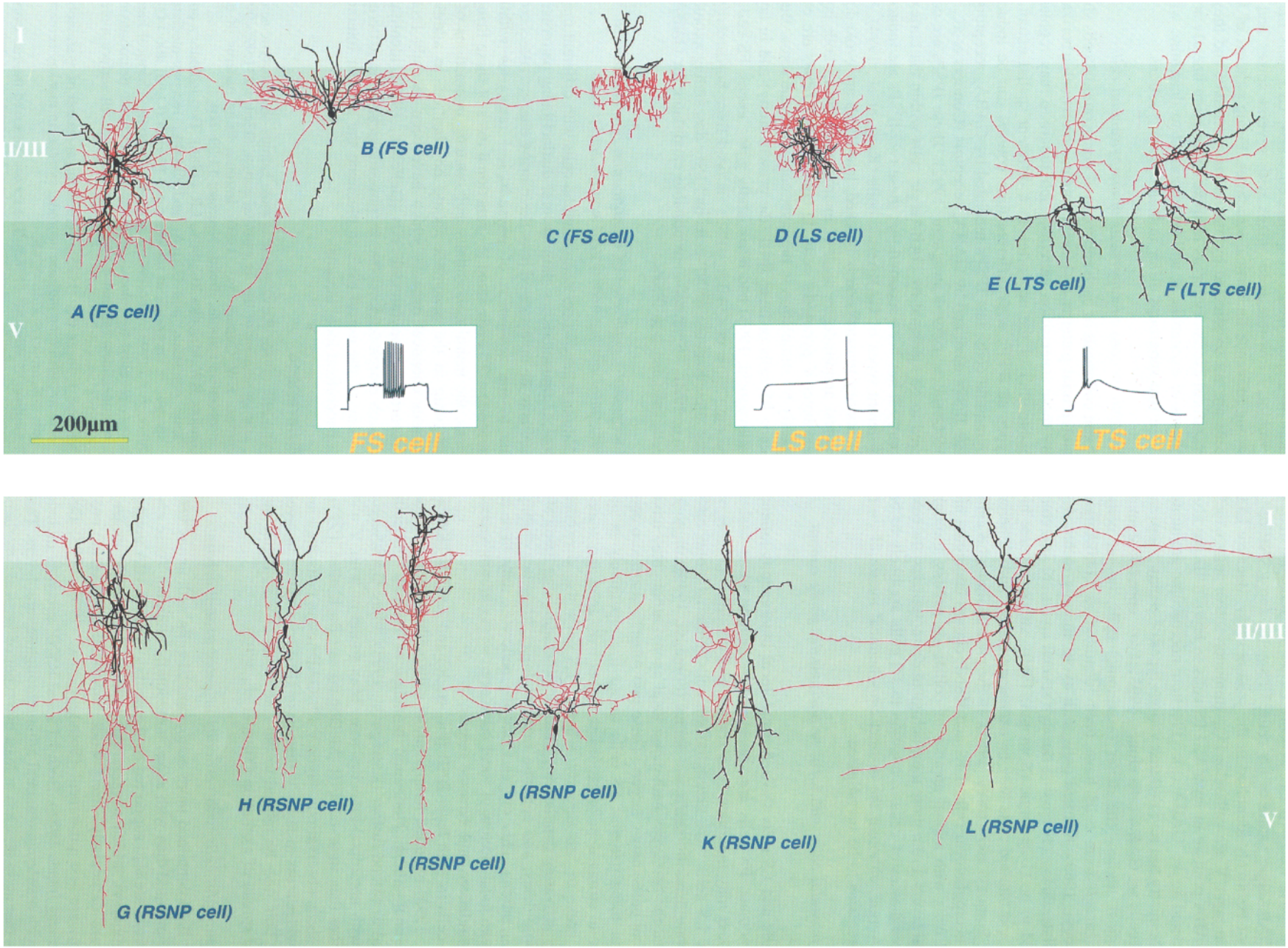
I
II/III
V
A (FS cell)
B (FS cell)
C (FS cell)
D (LS cell)
E (LTS cell)
F (LTS cell)
200µm
FS cell
LS cell
LTS cell
G (RSNP cell)
H (RSNP cell)
I (RSNP cell)
J (RSNP cell)
K (RSNP cell)
L (RSNP cell)

munoreactive for GABA in neocortex (Celio, 1986; this study). The GABAergic nature of LS cells, LTS cells, and RSNP cells was not positively identified in the present study. Because LTS cells in layer V are calbindin $D_{28k}$–immunoreactive cells which are GABA positive in layer V, LTS cells in layer II/III are also considered to be GABAergic. Electron microscopic immunocytochemistry has revealed that various types of aspiny nonpyramidal cells are GABA cells (Jones, 1993). From correlative morphological studies, chandelier (axoaxonic) cells, basket cells, and neurogliaform cells have been identified as GABAergic (Somogyi, 1989). Bitufted cells with axons running in arcades of collaterals loosely passing through several layers are also considered to be GABAergic (Somogyi, 1989), although some bipolar and bitufted cells may be excitatory (Peters and Kimerer, 1981; Somogyi and Cowey, 1981). In the present study, LS cells were neurogliaform cells. LTS and RSNP classes contained bitufted cells with axonal arcades of collaterals passing through several layers. From these morphological characteristics, the other three classes of cells in addition to FS cells are likely to be GABAergic, although the distinct cytochemical nature of each class remains to be investigated.

*Nonpyramidal cells with local or horizontally going axonal arbors*

FS cells and LS cells showed dense local innervations around their somata. FS cells are considered to include some basket cells and may innervate both somata and dendrites (Somogyi, 1989). LS cells were neurogliaform cells. Neurogliaform cells innervate dendritic shafts and spines (Somogyi, 1989), suggesting that the two types with dense local axonal arbors may have different postsynaptic targets. These two subgroups are also distinct in firing patterns: FS cells would fire repetitively in response to strong depolarizations at higher frequency and sometimes cease to fire abruptly, whereas LS cells would exhibit slowly activating depolarizing intrinsic potentials, start firing after some delay, and continue firing at lower frequency during depolarizations. This suggests that the neocortex may have at least two local circuits of focal inhibitions with different input–output relations and synaptic targets.

FS cells in both layer II/III (this study) and layer V (Kawaguchi, 1993) included nonpyramidal cells with horizontally going axonal arbors. Horizontal branches of layer V FS cells seemed to extend further (Kawaguchi, 1993). More GABAergic cells with horizontal branches have been found in layer V and VI rather than in layer II/III (McDonald and Burkhalter, 1993). From these observations, layer V FS GABAergic cells may inhibit wider areas in layer V than layer II/III FS cells do in layer II/III. This may be related to the role of layer V in regulating spatial spread of excitation (Silva et al., 1991).

*Nonpyramidal cells with vertically oriented axonal arbors*

Layer II/III contained more nonpyramidal cells with axons vertically oriented than with axons horizontally oriented. These observations are also supported by the studies of $^3$H-GABA uptake and transport, which suggest that vertical GABAergic projections are particularly strong while horizontal GABAergic projections are less prominent (Somogyi et al., 1981, 1983; DeFelipe and Jones, 1985). Both LTS and RSNP subtypes include cells with interlaminar axonal arbors through several layers. This means that neocortex has at least two types of vertical (interlaminar) connections originating from nonpyramidal cells with different firing patterns. When membrane potentials are shifted from hyperpolarized to depolarized states, LTS cells may fire prominent low-threshold spikes with several spikes and have strong influence on vertical structures. Firing patterns of RSNP cells are not so affected by membrane potentials, and they may transform excitatory inputs to spike firing more linearly at early phases of excitation. It will be important to determine whether these two subgroups differ in their synaptic actions.

*Synaptic actions of subgroups of nonpyramidal cells*

Axon collaterals of each subgroup of nonpyramidal cells showed preferential patterns of local, laminar, or vertical arborizations. By these innervation patterns, each subgroup may regulate the excitability of the neocortex to a different spatial extent. Two types of IPSPs with different time courses can be induced in pyramidal cells: fast IPSPs mediated by $GABA_A$ receptors, and late IPSPs mediated by $GABA_B$ receptors (Connors et al., 1988; McCormick, 1989; Kawaguchi, 1992). These IPSPs are considered to be mediated by GABAergic cells within the cortex. Recently it has been reported that these two IPSPs are induced by different types of GABAergic cells (Kang et al., 1994). When excitatory transmission is blocked, late IPSPs are evoked at the largest amplitude by layer II microstimulation in both layer II and layer V pyramidal cells. In contrast, fast IPSPs are evoked mostly by stimulation in the layer containing the soma. Because some FS cells in layer II/III (the present study) and in layer V (Kawaguchi, 1993) had horizontally going axons, FS cells may be the source of $GABA_A$ IPSPs induced from horizontally distant sites. Because RSNP cells had long descending axons from layer II/III, RSNP cells are possible candidates for GABAergic cells inducing late IPSPs.

*Functional significance of identification of physiological subgroups among neocortical nonpyramidal cells*

Although neocortical nonpyramidal cells with different morphological characteristics show several distinct firing patterns, it remains to be investigated how these firing characteristics contribute to the generation of physiological responses within the neocortex. To understand the functional roles of these firing patterns, the neural connections and synaptic interactions of each subgroup in the neocortex should be clarified. In addition to various chemical markers which have been recently found in neocortical nonpyramidal cells (DeFelipe, 1993), identification of each morphological class by physiological firing patterns will be one of the useful tools to elucidate the cellular interactions at neocortical local circuits.

## References

Celio MR (1986) Parvalbumin in most gamma-aminobutyric acid-containing neurons of the rat cerebral cortex. Science 231:995–997.

Connors BW, Gutnick MJ (1990) Intrinsic firing patterns of diverse neocortical neurons. Trends Neurosci 13:99–104.

Connors BW, Malenka RC, Silva LR (1988) Two inhibitory postsynaptic potentials, and $GABA_A$ and $GABA_B$ receptor-mediated responses in neocortex of rat and cat. J Physiol (Lond) 406:443–468.

DeFelipe J (1993) Neocortical neuronal diversity: chemical heterogeneity revealed by colocalization studies of classic neurotransmitters, neuropeptides, calcium-binding proteins, and cell surface molecules. Cereb Cortex 3:273–289.

DeFelipe J, Jones EG (1985) Vertical organization of γ-aminobutyric acid-accumulating intrinsic neuronal systems in monkey cerebral cortex. J Neurosci 5:3246–3260.

Donoghue JP, Wise SP (1982) The motor cortex of the rat: cytoarchitecture and microstimulation mapping. J Comp Neurol 217:390–404.

Fairén A, DeFelipe J, Regidor J (1984) Nonpyramidal neurons: general account. In: Cerebral cortex, Vol 1, Cellular components of the ce-

rebral cortex (Peters A, Jones EG, eds), pp 201–253. New York: Plenum.

Feldman ML, Peters A (1978) The forms of non-pyramidal neurons in the visual cortex of the rat. J Comp Neurol 179:761–794.

Foehring RC, Lorenzon NM, Herron P, Wilson CJ (1991) Correlation of physiologically and morphologically identified neuronal types in human association cortex *in vitro*. J Neurophysiol 66:1825–1837.

Hendry SHC, Schwark HD, Jones EG, Yan J (1987) Numbers and proportions of GABA-immunoreactive neurons in different areas of monkey cerebral cortex. J Neurosci 7:1503–1529.

Hendry SHC, Jones EG, Emson PC, Lawson DEM, Heizmann CW, Streit P (1989) Two classes of cortical GABA neurons defined by differential calcium binding protein immunoreactivities. Exp Brain Res 76:467–472.

Houser CR, Hendry SHC, Jones EG, Vaughn VE (1983) Morphological diversity of immuno-cytochemically identified GABA neurons in monkey sensory–motor cortex. J Neurocytol 12:617–638.

Jones EG (1975) Varieties and distribution of non-pyramidal cells in the somatic sensory cortex of the squirrel monkey. J Comp Neurol 160:205–268.

Jones EG (1984) Neurogliaform or spiderweb cells. In: Cerebral cortex, Vol 1, Cellular components of the cerebral cortex (Peters A, Jones EG, eds), pp 409–418. New York: Plenum.

Jones EG (1993) GABAergic neurons and their role in cortical plasticity in primates. Cereb Cortex 3:361–372.

Kang Y, Kaneko T, Ohishi H, Endo K, Araki T (1994) Spatio-temporally differential inhibition of pyramidal cells in the cat motor cortex. J Neurophysiol 71:280–293.

Kawaguchi Y (1992) Receptor subtypes involved in callosally-induced postsynaptic potentials in rat frontal agranular cortex *in vitro*. Exp Brain Res 88:33–40.

Kawaguchi Y (1993) Groupings of nonpyramidal and pyramidal cells with specific physiological and morphological characteristics in rat frontal cortex. J Neurophysiol 69:416–431.

Kawaguchi Y, Kubota Y (1993) Correlation of physiological subgroupings of nonpyramidal cells with parvalbumin- and calbindin$_{D28k}$-immunoreactive neurons in layer V of rat frontal cortex. J Neurophysiol 70:387–396.

Kawaguchi Y, Kubota Y (1995) Local circuit neurons in the frontal cortex and the neostriatum. In: Functions of cortico-basal ganglia loop (Kimura M, Graybiel AM, eds), in press. Tokyo: Springer.

Kubota Y, Hattori R, Yui Y (1994) Three distinct subpopulations of GABAergic neurons in rat frontal agranular cortex. Brain Res 649: 159–173.

Lund JS, Lewis DA (1993) Local circuit neurons of developing and mature macaque prefrontal cortex: Golgi and immunohistochemical characteristics. J Comp Neurol 328:282–312.

McCormick DA (1989) GABA as an inhibitory neurotransmitter in human cerebral cortex. J Neurophysiol 62:1018–1027.

McCormick DA, Connors BW, Lighthall JW, Prince DA (1985) Comparative electrophysiology of pyramidal and sparsely spiny stellate neurons of the neocortex. J Neurophysiol 54:782–806.

McDonald CT, Burkhalter A (1993) Organization of long-range inhibitory connections within rat visual cortex. J Neurosci 13:768–781.

Peters A (1984a) Chandelier cells. In: Cerebral cortex, Vol 1, Cellular components of the cerebral cortex (Peters A, Jones EG, eds), pp 361–380. New York: Plenum.

Peters A (1984b) Bipolar cells. In: Cerebral cortex, Vol 1, Cellular components of the cerebral cortex (Peters A, Jones EG, eds), pp 381–407. New York: Plenum.

Peters A, Jones EG (1984) Classification of cortical neurons. In: Cerebral cortex, Vol 1, Cellular components of the cerebral cortex (Peters A, Jones EG, eds), pp 107–121. New York: Plenum.

Peters A, Kimerer LM (1981) Bipolar neurons in rat visual cortex: a combined Golgi–electron microscope study. J Neurocytol 10:921–946.

Peters A, Kara DA, Harriman KM (1985) The neuronal composition of area 17 of rat visual cortex. III. Numerical considerations. J Comp Neurol 234:218–241.

Silva LR, Amitai Y, Connors BW (1991) Intrinsic oscillations of neocortex generated by layer 5 pyramidal neurons. Science 251:432–435.

Somogyi P (1977) A specific axo-axonal interneuron in the visual cortex of the rat. Brain Res 136:345–350.

Somogyi P (1989) Synaptic organization of GABAergic neurons and $GABA_A$ receptors in the lateral geniculate nucleus and visual cortex. In: Neural mechanisms of visual perception (Lam DK-T, Gilbert CD, eds), pp 35–62. Texas: Portfolio.

Somogyi P, Cowey A (1981) Combined Golgi and electron microscopic study on the synapses formed by double bouquet cells in the visual cortex of the cat and monkey. J Comp Neurol 195:547–566.

Somogyi P, Cowey A (1984) Double bouquet cells. In: Cerebral cortex, Vol 1, Cellular components of the cerebral cortex (Peters A, Jones EG, eds), pp 337–360. New York: Plenum.

Somogyi P, Cowey A, Halasz N, Freund TF (1981) Vertical organization of neurons accumulating $^3$H-GABA in visual cortex of rhesus monkey. Nature 294:761–763.

Somogyi P, Cowey A, Kisvarday ZF, Freund TF, Szentagothai J (1983) Retrograde transport of γ-amino[$^3$H]-butyric acid reveals specific interlaminar connections in the striate cortex of monkey. Proc Natl Acad Sci USA 80:2385–2389.

Zilles K, Wree A (1985) Cortex: areal and laminar structure. In: The rat nervous system, Vol 1, Forebrain and midbrain (Paxinos G, ed), pp 309–336. Sydney: Academic.